Behavior of RC Wide Beams under Eccentric Loading

Samer Magdy Mahmoud [1], Rasha T. S. Mabrouk [1*], Magdy E. Kassem [1]

[1] Structural Engineering Department, Faculty of Engineering, Cairo University, Egypt.

Abstract

Wide beams are one of the widely used structural elements in RC buildings due to the many special features that characterize them. The main objective of this research is to investigate the behavior of wide shallow beams under the effect of eccentric loading acting along their cross sections. To achieve that, an experimental program that consisted of seven wide beams was conducted. All beams were loaded using two concentrated loads at their middle third where the main parameters considered were: the magnitude of the load eccentricity, the longitudinal spacing between shear reinforcement, and the arrangement of the longitudinal reinforcement. Following that, a finite element analysis was performed where the analytical model used was first verified using the data from the experimental program. The results from both the experimental and analytical programs were in good agreement. Then, the finite element analysis was extended through a parametric study where other variables were studies such as the compressive strength of concrete, the transverse spacing between stirrups and the longitudinal reinforcement ratio. The results showed that the value of the load eccentricity, spacing between shear reinforcement, the arrangement of the main reinforcement along the beam cross section, and the compressive strength of concrete significantly affected the torsional resistance of shallow wide beams. Conclusions and recommendations are presented which can be useful for future researchers.

Keywords: Shallow Wide Beam; Torsional Moment; Cracks Pattern; Eccentric Load; Ultimate Load; Finite Element.

1. Introduction

Using wide shallow beams presents a good solution for many architectural obstructions as it provides a better height clearance and more simplicity for internal partitioning, this is in addition to removing the potential obstacles in the way of electromechanical ductworks. Also, wide beams save construction time due to the simplicity of formwork and reinforcement detailing [1]. Generally, shear stresses are produced in any reinforced concrete cross section through shear forces or/and torsion moments. Shear failure in concrete structures is catastrophic and happens suddenly, so it is a main concern for the design engineers. Once the tensile cracks occur in a beam, the shear capacity is reduced, so the designers control this issue by using conventional stirrups. On the other hand, the torsion stresses are always related to shear stresses which can be introduced to concrete structure by eccentric loading or eccentric support. It can clearly be seen in curved beams, spandrel beams and irregularly shaped sections. Practical situations where torsion in beams occurs are quite numerous, for example, when partitions or walls do not coincide with the centroidal longitudinal axis of the beam. This can occur in narrow beams but can be even more pronounced in wide beams due to their large width. Additionally, floor slabs cast monolithically with beams can cause torsional moments when they deflect under load. Torsion stresses lead to spiral or oblique cracks that extend all over the element which also can be improved or overcome by using well distributed vertical stirrups and main reinforcement steel bars that decrease the deflection and hair cracks, increase the ultimate load of failure, tensile strength, and ductility [2].

---

* Corresponding author: yrasha@yahoo.com

Recently, most of the experimental and analytical investigators focused on studying the wide shallow beams in terms of their shear behavior. One of the most widely investigated topic is the effect of shear reinforcement on the shear strength of the wide beams. Kamal [3] studied the effect of shear reinforcement through three different parameters which are the volumetric ratio of vertical stirrups, concrete compressive strength, and beam width. He concluded that the vertical stirrups contribute greatly to the shear strength of wide beams. Said & Elrakib [4] tested nine wide beams with varying spacing and diameter of vertical stirrups as well as having different yield stresses. They showed that using shear reinforcement considerably enhances the shear capacity and ductility of wide beams, and that using high grade steel is more effective than mild steel. Mohammadyan-Yasouj et al. [5] conducted an experimental program on six wide beams to study the use of different types of shear reinforcement. Vertical stirrups, independent bent bars, independent mid-depth horizontal bars, and a combination between bent up bars and vertical stirrups were used in this study. Ehab [6] carried out an experimental program to study the effect of shear reinforcement on the shear behavior and modes of failure of wide shallow beams. Four different parameters including shear reinforcement ratio, shear span to depth ratio, spacing between vertical stirrups, and number of vertical branches were investigated. The results showed that the vertical stirrups have a great contribution to the shear strength, ductility, and width of shear cracks. Transverse spacing between stirrups was proven to have a considerable effect on the shear strength of wide beams as shown by Lubell et al. [7]. While Shuraim [8] conducted a vast study on 16 two span continuous wide beams with various arrangement of stirrups in the transverse direction. He concluded that using four branch stirrups was more effective than two legged ones for the same amount of stirrups. Elanasry et al. [9] suggested an innovative system of shear reinforcement for wide beams using confined spiral stirrups. They studied variable parameters of the stirrups such as spacing and ratio of stirrups. They also studied the effect of changing the longitudinal reinforcing bars on the behavior of the beams.

Concerns regarding design code formulation for shear in wide beams have been extensively studied. Angelakos et al. [10] investigated shear provisions provided by the ACI code [11] and showed that they can be quite un-conservative in the case of large beams or thick slabs. Sherwood et al. [12] conducted an experimental program to study the validity of the ACI-05 [13] recommendations. They stated that "the width of a member does not significantly affect the shear stress at failure and that the ACI 318-05 [13] provisions requiring different shear capacities for slabs, wide beams, and narrow beams are not appropriate." Kim et al. [14] proposed an equation to calculate the shear strength of slabs depending on the spacing and support conditions. Collins et al. [15] studied the shear behavior of thick slabs without shear reinforcement. They found that the ACI code [16] provisions are highly underestimated in this case and that using minimum shear reinforcement improves the behavior of such thick slabs.

Torsion of reinforced concrete beams has been the topic of study for many years [17, 18]. Fang et al. [19] studied the size effect with regards to torsion in beams with and without stirrups. The properties of concrete as well as reinforcement generally affect the capacity of beams in torsion. Fang et al. [19] studied beams subjected to pure torsion using both normal and high strength concrete. They concluded that using high strength concrete improved the capacity and the cracked stiffness of the beams in torsion. On the other hand, Kim et al. [20] studied the effect of using stirrups with high strength reinforcement to resist torsional stresses in beams. They concluded that using high strength reinforcement in this case leads to lower capacity than the design values. Also, Lee et al. [21] studied the maximum torsion reinforcement with comparison between the different design codes regarding their accuracy. Different beam shapes were also studied, for example, Jeng et al. [22] studied large size hollow sectioned beams. Ju & Lee [23] studied the combined effect of torsion and bending. They tried to simulate the behavior of the beams under these stresses through an analytical model and comparison with previous experimental data.

2. Significance and Layout of the Research Program

Based on the above, considerable research was performed on either wide beams or the torsion behavior of narrow beams. However, scarce work can be found on the study of wide beams subjected to torsional effects. The main objective of this research is to study the effect of applying eccentric loading on shallow wide beams thus exerting torsional moments that lead to shear stresses and how the behavior is affected by changing different parameters through experimental as well as analytical analysis. The parameters under study were decided as those mostly affecting the wide beams or the torsion behavior of beams as reported in the literature; mainly the eccentricity of the load, the vertical stirrups spacing in the longitudinal direction and in the transverse direction, the arrangement of main longitudinal reinforcement, the compressive strength of concrete, and the ratio of the main longitudinal reinforcement. Torsion does not usually occur without any other action and thus the beams were all subjected to the combined action of torsion, shear, and bending through a two-point loading setup.

Figure 1 shows the layout of the research program. It is mainly divided into two parts namely the experimental program and the analytical one. The experimental program consists of testing seven wide shallow beam specimens under two-point loading and the numerical analysis was conducted through the finite element program ANSYS V.19 [24]. In the finite element analysis, first the seven specimens tested before were modeled for verification of the soundness of the modeling procedure used and then a parametric study was conducted to further understand the behavior of the wide beams in under eccentric loading.
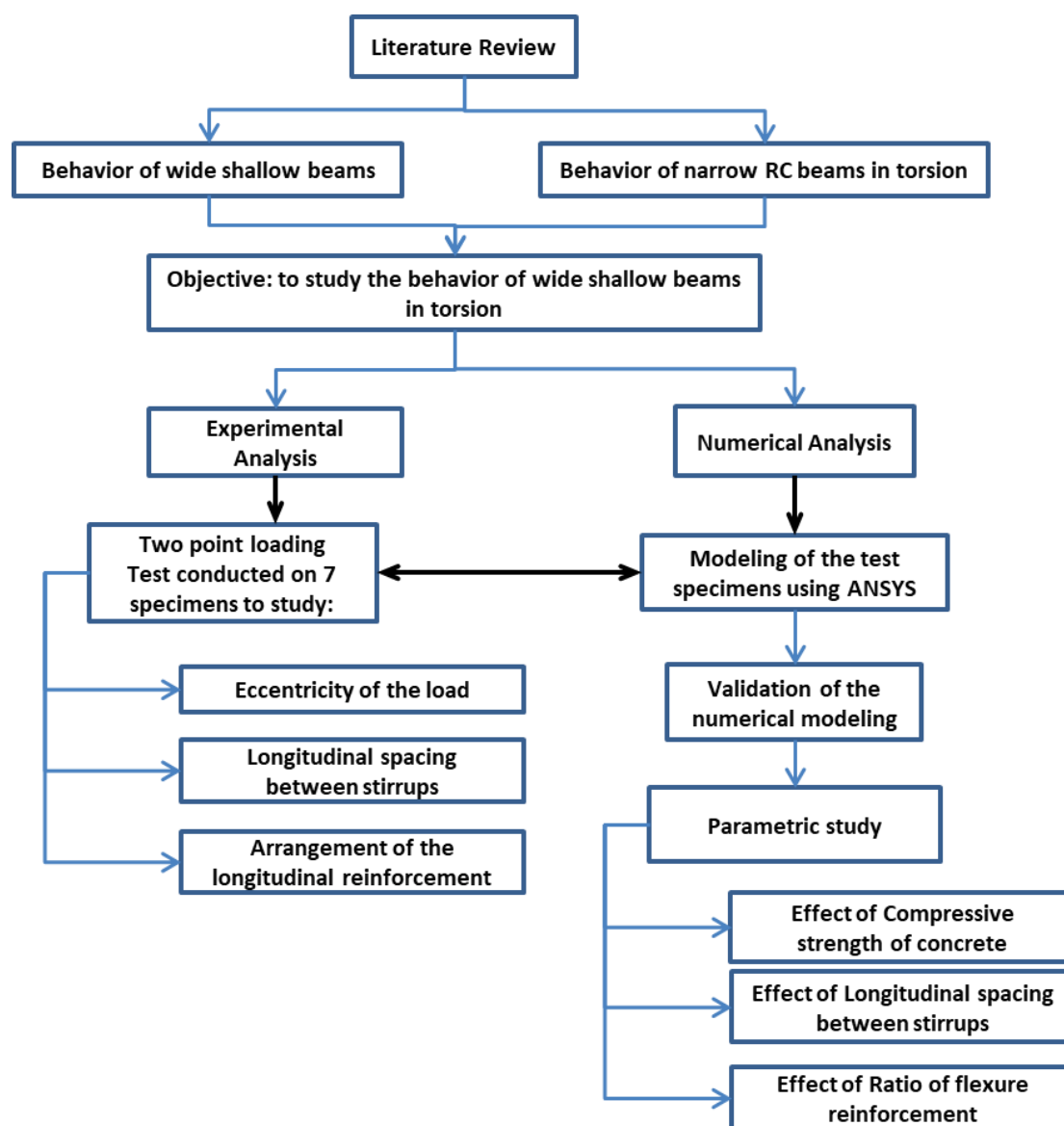
Figure 1. Layout of the research program

3. Experimental Program

3.1. Specimens

The experimental program consisted of seven wide shallow beam specimens. A summary of the details of all beams is shown in Table 1. The loading setup was designed to introduce torsional moments on the specimens through the application of two vertical concentrated loads with varying eccentricities (e) of zero, 100 mm and 200 mm. These values correspond to e/B = zero, 0.167 and 0.333 where B is the width of the beam. The two-point loads were applied at the two middle thirds of the longitudinal span. All beams were casted and tested at the Concrete Research Laboratory, Faculty of Engineering, Cairo University. The seven specimens had the same cross section of 600×200 mm and the same span of 1700 mm with a clear span of 1500 mm. The clear concrete cover was 20 mm giving a beam depth d=180 mm. The ratio of the main bottom longitudinal reinforcement was taken as 0.78% which satisfies the minimum and maximum ratios set by ECP 203-2018 [25] and ACI 318-19 [26]. Figure 2a shows the details of all beams in plan where "Front" herein refers to the longitudinal side of the beam closest to the point load and back refers to the other side. Figure 2b shows the typical longitudinal cross section. Different arrangements were used for the bottom reinforcement; uniform distribution with two different diameters and different number of bars namely 4 and 7 and then banded type where part of the reinforcing bars was concentrated at the same side as the loading as shown in Figure 2c, 2d and 2e. The latter arrangement was chosen based on reports from previous research that banded reinforcement arrangement showed improvement in the capacity of the wide beams [5]. The top reinforcement was 4 bars with the diameter 10 mm. Stirrups with four branches of diameter 6 mm were used. Design codes [25, 26] limit the spacing between stirrups in the longitudinal direction to d/2. Based on this, the spacing in the longitudinal direction was taken as 50, 75, 100 mm, thus covering a range less than and close to the maximum spacing stipulation.

Table 1. Summary of the details of the beam specimens

Specimen		Dimensions	e (mm)	e/B	Bottom Reinforcement				Stirrups	
					Area (mm²)	D (mm)	No. of bars	Spacing between the bars (mm)	No. of branches	s (mm)
Group (1)	B1		0	0	804.24	16	4	187		75
	B2		200	0.333	804.24	16	4	187		75
	B3		100	0.167	804.24	16	4	187		75
Group (2)	B4	600×200×1700 mm	200	0.333	804.24	16	4	187	Ø6 @ 187 mm - 4 branches	100
	B5		200	0.333	804.24	16	4	187		50
Group (3)	B6		200	0.333	791.68	12	7	93.33		75
	B7		200	0.333	791.68	12	7	187 93.33		75

e: Load eccentricity along the cross section of the beams, B: width of the beam;

D: Diameter of reinforcement steel bars, s: Spacing between stirrups along the span of the beams.

a) Plan

b) Sectional elevation

c) Cross section A-A for beams B1 to B5

d) Cross section A-A for beam B6

e) Cross section A-A for beam B7
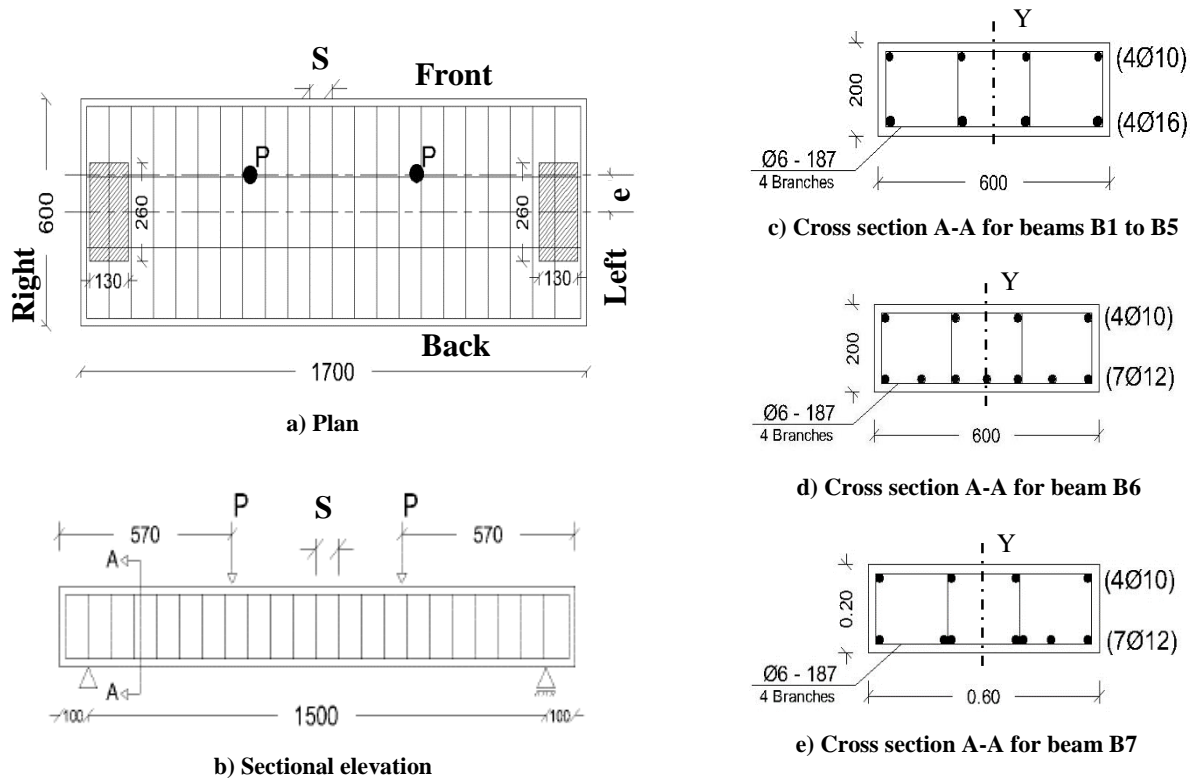
Figure 2. Specimen details for Beams B1 to B7 (All dimensions are in mm)

Figure 3. Loading test setup for all beams
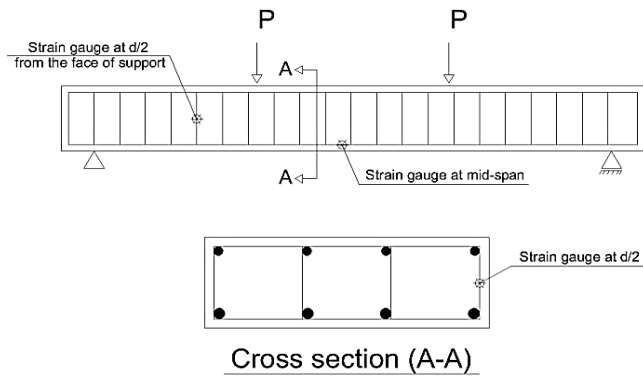
Figure 4. Location of Strain gauges for all specimens

The concrete mix was designed to give a characteristic compressive strength of 30 N/mm^2. Compressive strength tests were conducted on standard cubes and gave an average strength of 30.6 N/mm^2. The loading was performed by means of a steel frame composed of groups of steel girders tied together by high strength steel bolts and nuts as shown in Figure 3. The load cell used had a capacity of 1000 kN. Three LVDTs were used to measure the deflection of the specimens. One LVDT was placed at the mid span of the specimens and the other two one under each load. Electrical strain gauges were used to measure the strain in the longitudinal reinforcement where they were placed at the maximum flexure point at mid-span. Strain gauges were also used in the vertical leg of the stirrups at d/2 from the face of support as shown in Figure 4. The position of strain gauges in this case were chosen at the location where the shear cracks are most expected to occur.

The beams were divided into three groups to study three parameters as follows:

- Group (1): This group consists of three beams – B1, B2, B3 – designed to study the effect of the load eccentricity along the cross section of the beams (e) varying from zero for B1, 200 mm for B2 and 100 mm for B3.

- Group (2): This group consists of two beams – B4, B5 in addition to beam B2 – where the spacing between the stirrups in the longitudinal direction (s) is studied with the beams subjected to a fixed eccentricity (e/B) of 0.333.

- Group (3): This group consists of two beams – B6, B7 in addition to beam B2 – to the study the effect of the main longitudinal reinforcement arrangement as shown in Figure 2c through 2e.

3.2. Experimental Test Results

Table 2 shows the experimental output for all the beams in terms of the ultimate load, the first crack load, and the corresponding deflections as well as the calculated values of stiffness, ductility and toughness of each specimen and the modes of failure.

Table 2. Summary of the experimental results

Specimen		P_{cr} (kN)	P_u (kN)	Δ_{cr} (mm)	Δ_u (mm)	ε_{main} (μ)	ε_s (μ)	Stiffness (kN/mm)	Ductility factor	Toughness (kN.mm)	Mode of failure
	B1	80	320	1.1	14.5	4828	142	29.4	2.17	3426.8	Flexure
Group (1)	B2	110	260	5.2	19.8	2568	1179	15.5	1.56	3720.6	Flexure - Torsion
	B3	85	330	4.2	21.2	4828	264	19.1	1.91	4441.9	Flexure - Torsion
Group (2)	B4	90	250	5.5	18.6	2158	493	13.4	N/A	2678.8	Torsion
	B5	90	290	2.8	20.8	2481	333	18.6	1.88	4241.6	Flexure - Torsion
Group (3)	B6	90	220	4.9	16.5	2033	693	15.2	N/A	2214.1	Torsion
	B7	90	250	4.2	14.1	2460	391	20.0	1.00	2015.0	Torsion

P_{cr}: Load at first crack, P_u: Ultimate Load;

Δ_{cr}: Deflection at first cack load, Δ_u: Deflection at ultimate load;

ε_{main}: Strain in longitudinal reinforcement at failure, ε_s: Strain in stirrups at failure.

Cracking Patterns

The behavior of all specimens was observed under loading increments until failure and the cracking patterns were detected and marked. For ease of reference the notation front face was used for the beam side closer to the load as mentioned before. Figure 5 shows the cracking pattern after failure for the control beam B1 where the applied load was at the centerline of the specimen without any eccentricity. The first crack appeared at the center line of the

specimen on both the front and the back sides at approximately the same time and it was a flexure vertical crack. At higher loading levels, the number of cracks increased, their widths increased, and they extended from the front side towards the back side through the bottom face until they were connected. There were no cracks observed on the upper or left and right sides. The final cracks at the front and back sides of the beam followed a similar pattern as shown in Figure 5a and 5c. This is in agreement with the beam having zero load eccentricity. Finally, the beam failed in flexure due to the excessive increase in flexure cracks.

The rest of the specimens B2 to B7 showed a different cracking pattern from B1. The six beams generally had similar crack patterns behavior. The typical final cracking pattern is shown in Figure 6 with Beam B2 shown as an example. The first crack observed was a vertical flexure crack that began to appear at the middle third of the specimen at the front side followed by the same type of crack at the back side. After that, these cracks started to extend horizontally at the bottom face of the specimens to be connected at the middle third region. At higher loading levels, some cracks inclined at 45° began to appear on the front face that extended to the bottom face near the support, then some inclined and horizontal cracks appeared on the top face near the supports that extended to both the left and right sides forming again cracks inclined at 45°. It can be seen from Figure 2a and 2b that the front face showed clearly inclined shear cracks while the back face had vertical widely uniformly spaced cracks. At the end of loading, a bundle of cracks was formed at the support zone till failure. These cracking patterns well indicate the presence of torsional moments.

a) Front face   b) Bottom face

c) Back face   d) Top face and side
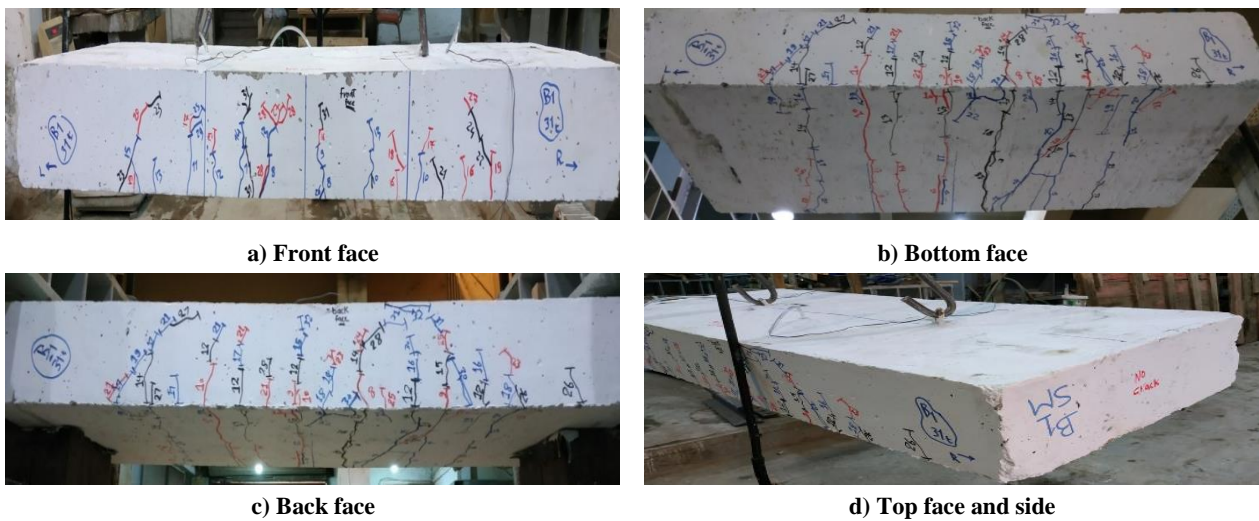
Figure 5. Cracking pattern for specimen B1

a) Front face   b) Right face

c) Back face   d) Left face

e) Bottom face   f) Top face
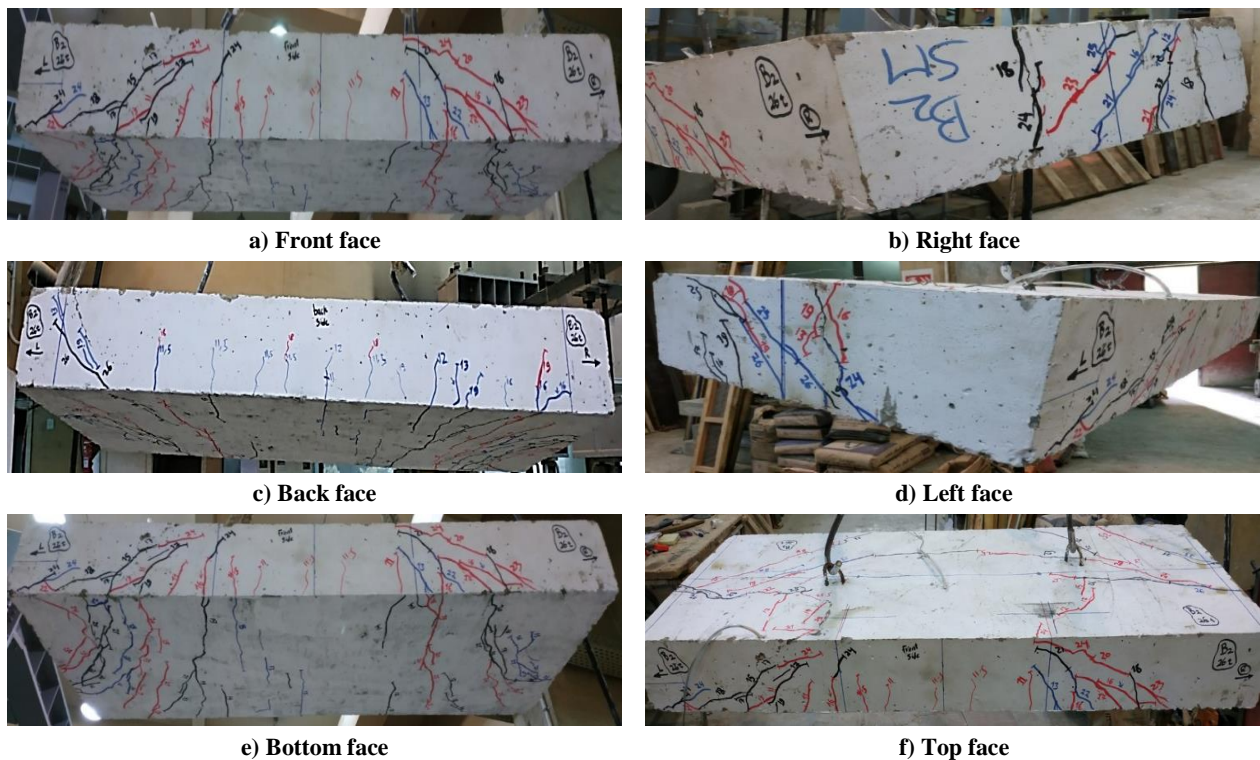
Figure 6. Cracking pattern for specimen B2

Figure 7 shows a comparison of the cracking pattern for the front face with the bottom one for Beams B2 to B7. As previously mentioned, these six beams showed a behavior typical for beams subjected to torsion. However, the effect of the parameters under study can be seen clearly in the variations between the beams. Comparing Beams B1, B2, and B3, as the load eccentricity increased, the number of cracks occurring in the middle third of the specimens decreased showing the least occurrence in Beam B2 with load eccentricity e/B=0.333. In addition, the diagonal cracks on the front face reached almost the full depth of the beams indicating torsional shear stresses and they were more pronounced in Beam B2. Beam B3 with eccentricity e/B=0.167 showed a crack pattern very similar to Beam B1 which was loaded without any eccentricity.

Beam B4 with the largest longitudinal spacing between stirrups (100 mm) showed more horizontal cracks on the bottom face than Beams B2 and B5 with spacing 75 and 50 mm, respectively. However, the inclined diagonal cracking patterns seen on the front face of the beams were different. In Beam B4, a clear distinct diagonal crack was seen on both sides of the span. While in Beam B2, a bundle of diagonal cracks was observed on both the left and right sides. As for Beam B5, the same two bundles were present however, the bundle width and the number of cracks within the bundle were higher than in case of Beam B2 and the cracks widths were lower. This larger number of cracks with smaller width in Beam B5 agrees well with it having the highest ductility factor among the three beams as shown in Table 2. Cracking pattern also showed dependency on the arrangement of the longitudinal reinforcement. Comparing the beams in Group (3), Beam B2 showed the largest number of diagonal cracks with the smallest widths followed by Beam B7 and then Beam B6 which showed two distinct diagonal cracks with larger width. This cracking pattern again correlates with Beam B2 showing the highest ductility behavior among the three beams.

The cracks on the back face for Beams B2, B4, B5 and B6 were vertical and rather widely dispersed with a uniform distribution along the length of the beam reaching only the mid depth of the beam. As for Beam B3 the cracks were also vertical but more closely dispersed and reaching almost the full length of the beam. The cracks at the back face for beam B7 were vertical in the middle third of the span and inclined towards the support at the two ends of the beam. These differences in the cracking patterns behaviors for the front and back faces confirm the occurrence of torsional stresses for beams B2 to B7.

a) Beam B2

b) Beam B3

c) Beam B4

d) Beam B5

e) Beam B6

d) Beam B7
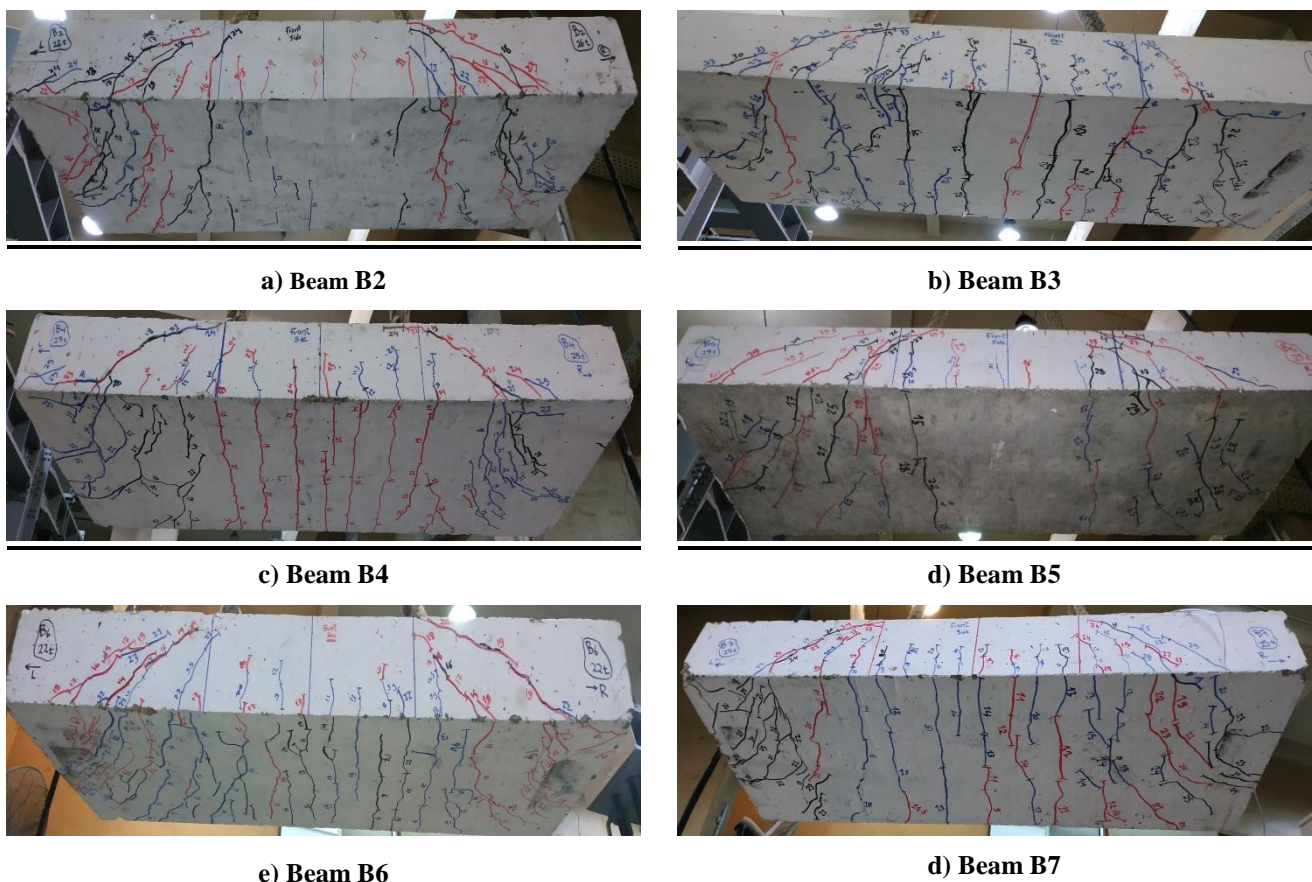
Figure 7. Cracking pattern for beam specimens B2 to B7 – Front face with bottom side

Load-Deflection Relationship

The applied load versus the vertical deflection at mid span for all the beams is shown in Figures 8 through 10. Figure 8 shows the results for Group (1). Beam B1 showed a bilinear curve shape while Beams B2 and B3 exhibited a non-linear behavior until failure. The first crack load was almost similar for Beams B1 and B3 but slightly higher for

Beam B2. Also, the results show that Beam B3 had the maximum ultimate load of 330 kN while Beam B2 showed the minimum ultimate load of 260 kN while Beam B1 gave a value of 320 kN. However, these readings do not reflect the actual behavior since the loading for Beam B1 was terminated due to safety issues before the beam reached its ultimate capacity. The curve representing Beam B1 could progress as shown in Figure 8 by the dotted line extended from point A, which is the final test reading, to point B, which can be considered the predicted ultimate failure load. According to that, Beam B1 was supposed to show a higher load capacity which is supported by the FEM calculations that will be shown later. The readings of Beams B2 and B3 show that the bigger the eccentricity of the load the lower ultimate load capacity due to the higher torsional moments exerted on the specimen. Comparing the deflection at ultimate load, Beam B2 showed a slightly lower value compared to Beam B3.

Group (2) was tested to show the effect of longitudinal spacing between stirrups on the behavior of each specimen. The load-deflection curves for specimen B2, B4, and B5 are shown in Figure 9 where the three specimens showed initial linear behavior followed by nonlinear load-deflection behavior up to failure. A slight increase of 4% occurred when the spacing between stirrups was decreased from 100 to 75 mm. However, a noticeable increase of 16% was obtained when the spacing was decreased from 100 to 50 mm. As for the deflection at ultimate load, Beam B2 (75 mm spacing) showed a value of 19.8 mm, Beam B4 (100 mm spacing) shows minimum deflection of 18.6 mm while Beam B5 (50 mm spacing) showed the maximum deflection of 21.2 mm.

The load-deflection curves for Group (3) are shown in Figure 10. The three beams B2, B6 and B7 were designed to have the same bottom reinforcement ratio value of 0.78% but with different reinforcement arrangements as shown in Figure 2c, 2d and 2e where Beams B2 and B7 had uniform bar distribution but with different diameters while for Beam B7 the reinforced bars were concentrated on the side under the load. The values of the ultimate load obtained from the loading test were different despite having the same reinforcement ratios where Beam B2 showed the highest value of 260 kN followed by Beams B7 and then B6 gave the lowest value of 220 kN. To quantitatively explain this behavior, the values of the cracked moments of inertia (I) for the half section under load around the center line of the cross sections Y shown in Figure 2c, 2d and 2e, were calculated using equation 1. The values of the moment of inertia calculated were the highest value for Beam B2 and the lowest value for Beam B6. Comparing the values of the ultimate load for the corresponding beams, the values for the ultimate load follow the same pattern as shown in Figure 11. This means that behavior of the specimens is affected by the reinforcement distribution even if the reinforcement ratio is kept constant with the ultimate load value increasing as the moment of inertia increases.

$$I = [\gamma \, (\boldsymbol{\pi} \, D^2)/4] . (\textstyle\sum r_i^2) = K \, D^2 . (\textstyle\sum r_i^2) \tag{1}$$

Where $K = \gamma \, \boldsymbol{\pi}/4$

I: Cracked moments of inertia γ: density of steel, D: diameter of the reinforcing bar, r_i: distance measured from the center line of the steel bar to the center line of the cross section of the beam.

Strain in Stirrups

The values of the strain in the stirrups for the seven beams are shown in Table 2. Beam B2 had the maximum strain value of approximately 1180 micro-strain while the other six beams gave strain values ranging between 132 to 694 micro-strain. The strain measured in stirrups shows some discrepancies. This can be explained since the local strain in the leg of the stirrup is greatly affected by its location with respect to the cracks. For each beam, a strain gauge was located at d/2 from the face of the support; however, this position relative to the cracks induced can be different from one specimen to the other and could not be unified. In general, the web reinforcement did not reach its yield limit as the yield strain for bars with diameter 6 mm steel is 1690 micro-strain.

Strain in Longitudinal Reinforcement and Modes of Failure

The load strain curves for the longitudinal reinforcement for all the tested beams are shown in Figures 12 through 14. The yield strain for steel bars diameter 16 mm and 12 mm is 2330 micro-strain and 2475 micro-strain, respectively. For Group (1) with different eccentricity ratios, the longitudinal reinforcement in the three beams B1, B2, and B3 reached the yield limit before concrete crushing at 250, 240, and 270 kN, respectively. It can be seen from Figure 12 that Beams B2 and B3 showed very similar load strain behavior, where the yielding of main reinforcement is very clear through a bilinear curve. This shows that beams having low eccentricity values exhibit behavior close to that of beams without any eccentricity. For Group (2), Beams B2 and B5 with lower spacing between stirrups reached the yield limit at 240 and 280 kN while the longitudinal reinforcement of B4 with spacing of 100 mm did not reach the yield limit. This shows that the lower spacing between stirrups leads to a better ductile behavior and mode of failure in addition to higher ultimate load values. For Group (3), where the longitudinal reinforcement distribution was studied, Beam B2 with uniform distribution and higher bar diameter giving higher cracked moment of inertia showed yielding in the main reinforcement. While for Beams B6 and B7, changing the reinforcement distribution to non-uniform or lowering the area of the individual bar diameter showed a rather non-ductile behavior with the bars in Beam B6 not reaching the yield limit and those in B7 almost reaching the yield strain with a value of 2460 micro-strain.
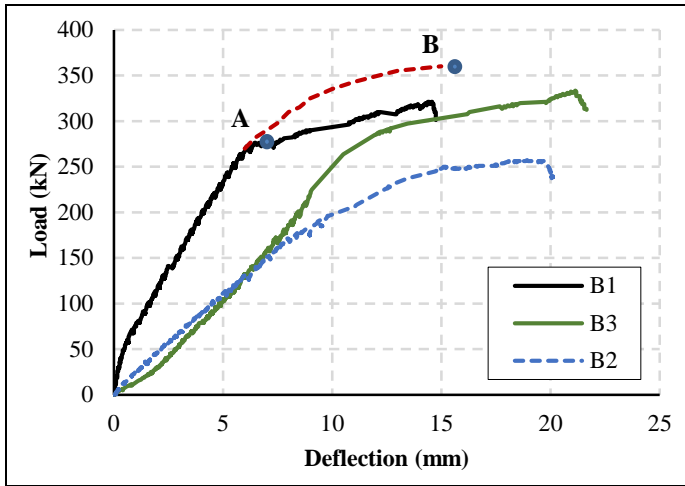
Figure 8. Load-Deflection curves for Group (1)
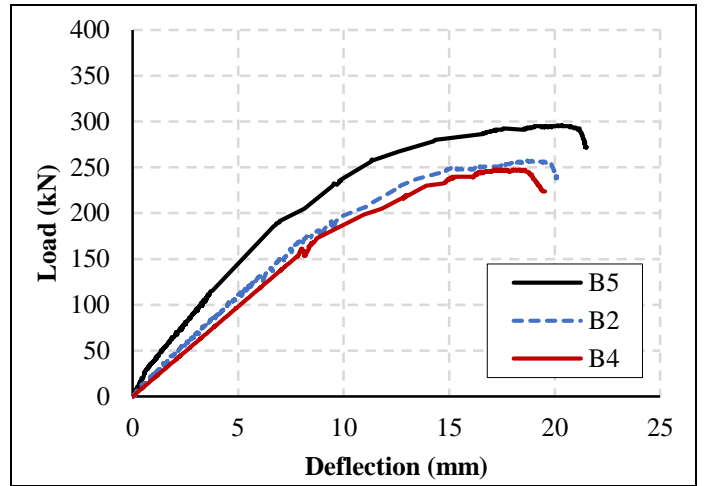
Figure 9. Load-Deflection curves for Group (2)
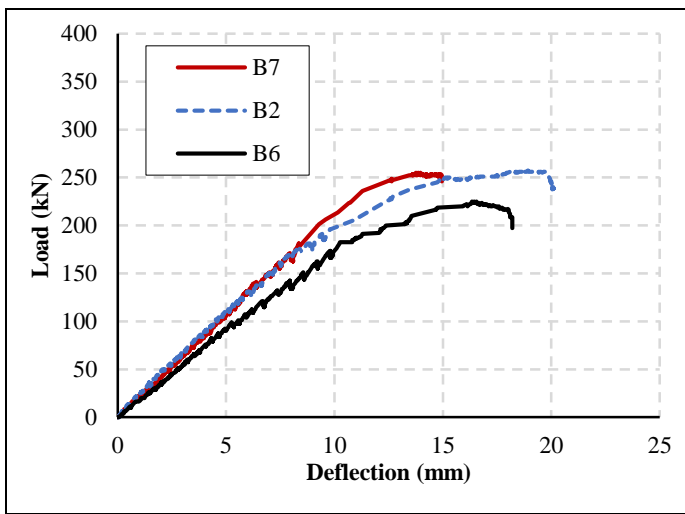
Figure 10. Load-Deflection curves for Group (3)
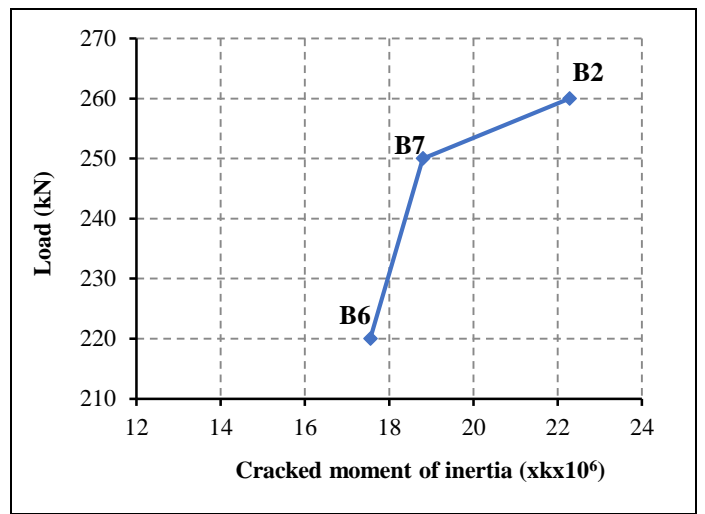
Figure 11. Effect of bottom reinforcement distribution
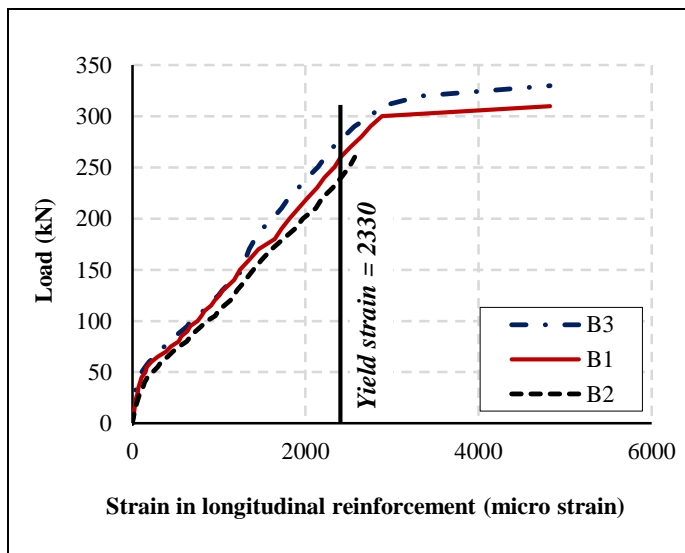
Figure 12. Load-Strain curves for longitudinal reinforcement – Group (1)
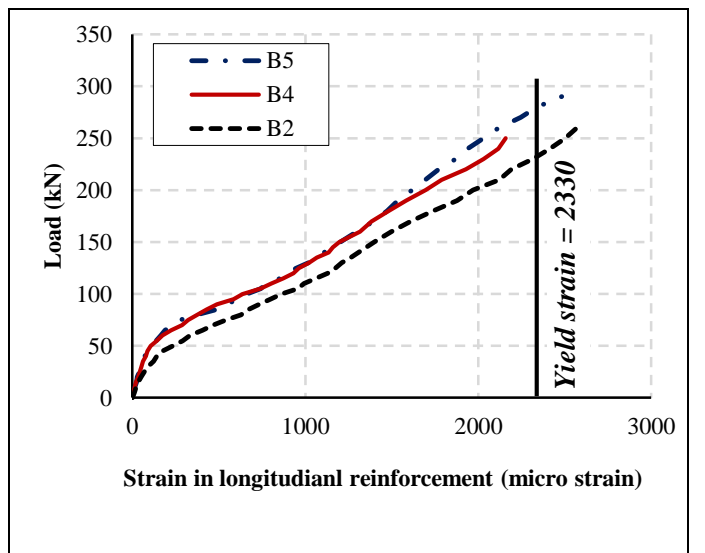
Figure 13. Load-Strain curves for longitudinal reinforcement – Group (2)
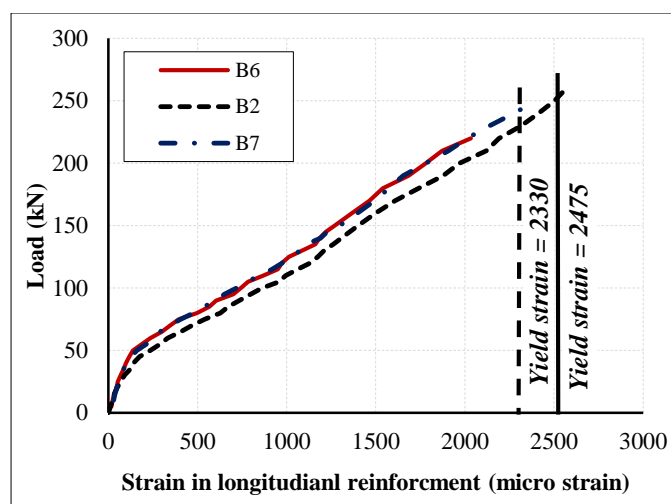
Figure 14. Load-Strain curves for longitudinal reinforcement – Group (3)

Beam B1 failed in flexure with the main reinforcement clearly reaching the yield strain as shown in Figure 12. As for beam B3, flexural failure was considered based on the shape of the load strain curve despite the shear torsional cracks observed. Beams B2, and B5 showed yielding in the main reinforcement just before failure leading to a combined flexure torsion failure mode while reinforcement in Beam B6 almost reached the yield strain at failure. On the other hand, the longitudinal reinforcement in Beams B4 and B6 did not reach the yield limit and failed due to torsional stresses. Beam B4 showed the most pronounced torsional shear failure where it failed suddenly, and the diagonal cracks was very dominant.

Structural Behavior

Stiffness is the ability of the specimens to resist the deformation in response to the applied force where the more flexible the specimens are, the less stiff they are [18]. The stiffness can be calculated as the slope of the linear part of the ascending branch of the load-deflection curve. While toughness is the ability of the material to absorb energy and deform plastically without any fracture, where toughness can be determined as the area under load-deflection curve up to specified level of failure [18].

Ductility is the ability of the material to undergo large deformation without rupture before failure, where ductility can be measured using several measures as displacement ductility factor, drift index and curvature-ductility factor [27]. Ductility of specimens was evaluated using the displacement ductility factor (μ_Δ) which is defined as the ratio of the mid span deflection at the ultimate load to the mid span deflection at the yield load.

It was noted that Beam B1 with zero eccentricity and 16 mm uniformly distributed longitudinal bars had the maximum stiffness of 29.4 kN/mm, while B4 with longitudinal spacing between stirrups of 100 mm, 200 mm eccentric load and 16 mm uniformly distributed longitudinal bars had the least stiffness of 13.4 kN/mm. As for toughness, B3 and B5 had the maximum values of toughness of 4440 and 4240 kN.mm respectively while B7 had the minimum value of toughness of 2010 kN.mm. B1 had the maximum ductility factor of 2.17. On the other hand, the rest of specimens showed a ductility factor that ranges from 1.00 to 1.91.

From Table 2, it can be seen that decreasing the eccentricity of load from 200 mm (B2) to zero (B1) for Group (1) improved the ductility by 39.1% and the stiffness by 89.6% while the toughness decreased by 7.9%. The decrease in the longitudinal spacing between stirrups from 100 mm (B4) to 50 mm (B5) lead to an increase in the stiffness by approximately 39%. The decrease in the spacing between stirrups also lead to a more ductile behavior and an increase in the toughness by 58.3% where this can be explained by the ability of a member to resist fracture due to the presence of stirrups with small spacing in the longitudinal direction. Finally, changing the distribution of longitudinal steel bars from uniform distribution to non-uniform concentrated distribution under load for Beams B6 and B7 increased stiffness by 31.5% and decreased the toughness approximately by 9%. Both beams showed a lower ductile behavior compared to B2.

4. Finite Element Analysis

The finite element analysis was conducted in two consecutive stages as shown in Figure 1. First, the seven tested specimens were modeled and analyzed using the finite element analysis program ANSYS V.19 [24]. Each element in the model was defined using a specified element type from the ANSYS library where concrete is defined using SOILD 65, steel reinforcement is defined using LINK 180 and steel plates are defined using SOILD 45 [24]. To ensure that

the model is acting similar to the experimental specimens, the boundary conditions were applied to simulate the actual conditions of the experiment where the supports were modeled in such a way that fixed supports were created by defining the values of the displacement in X, Y, and Z directions equal to zero and the rotation in X, Y, and Z directions also equal to zero. In this part, the model is assessed and compared with the data obtained from the experimental program to assure the validity and soundness of the model used.

The second part consisted of an extended parametric study where the study of different parameters was conducted to further understand the behavior of wide shallow beams under eccentric loading. Seven more beams were analyzed with varying parameters such as the compressive strength of concrete, the main reinforcement ratio, the spacing between the stirrups, and the number of branches of the stirrups used.

4.1. Comparison between Experimental Results and FEM analysis

The comparison between the experimental results and FEM analysis was conducted through cracking patterns, modes of failure, cracking loads, ultimate loads, load deflection curves, and load strain curves for transverse and longitudinal reinforcement. All numerical results obtained through the finite element analysis were compared with the experimental data shown in section 3.2.

Table 3. Summary of the FEM results for beams B1 to B7

Specimen		P'_{cr} (kN)	P'_u (kN)	Δ'_{cr} (mm)	Δ'_u (mm)	ε'_{main} (μ)	P'_{cr}/P_{cr}	P'_u/P_u	Δ'_{cr}/Δ_{cr}	Δ'_u/Δ_u	$\varepsilon'_{main}/\varepsilon_{main}$	Mode of Failure
Group (1)	B1	145	364.8	2.75	11.33	4323	1.80	1.14	2.5	0.78	0.90	Flexure
	B2	115	243.2	3.19	16.90	2407	1.04	0.94	0.61	0.85	0.93	Flexure - Torsion
	B3	115	298.6	2.10	16.42	3549	1.35	0.90	0.50	0.77	0.74	Flexure - Torsion
Group (2)	B4	91.3	204.5	3.26	18.15	2511	1.01	0.82	0.60	0.98	1.16	Flexure - Torsion
	B5	115	305.9	3.45	20.96	3493	1.27	1.05	1.23	1.01	1.41	Flexure - Torsion
Group (3)	B6	95	194.9	3.46	13.60	1474	1.06	0.89	0.64	0.82	0.73	Torsion
	B7	95	264.0	2.78	17.42	2204	1.06	1.06	0.66	1.24	0.90	Torsion
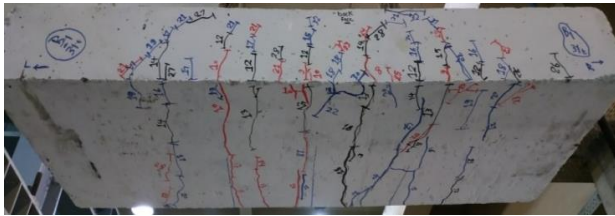
a. Experimental
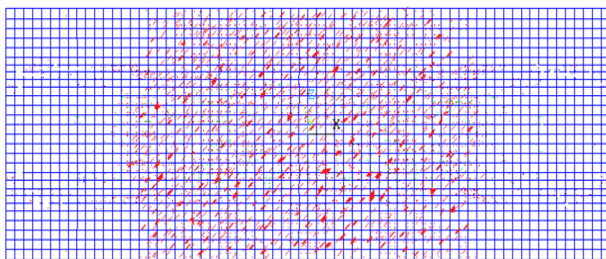
b. Analytical results from FEM Analysis– Bottom Face
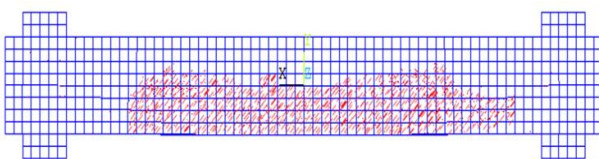
c. Analytical results from FEM Analysis – Front Face

Figure 15. Comparing cracking patterns for specimen B1
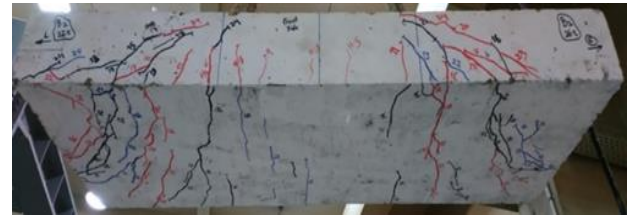
a. Experimental
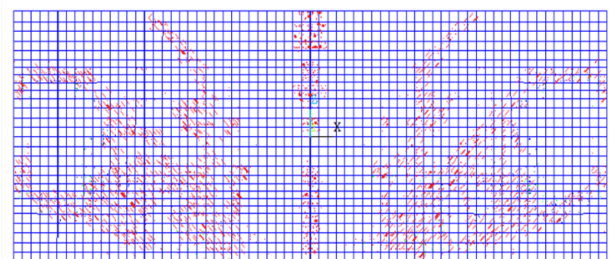
b. Analytical results from FEM Analysis– Bottom Face
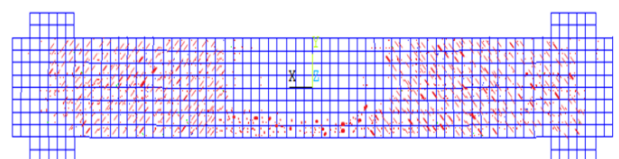
c. Analytical results from FEM Analysis – Front Face

Figure 16. Comparing cracking patterns for specimen B2
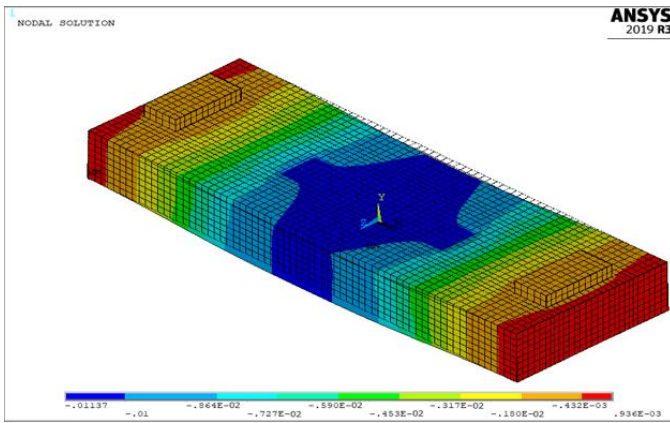
a) Top view
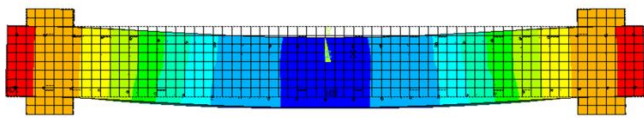
b) Front view

Figure 17. Deformation for specimen B1 - FEM Analysis
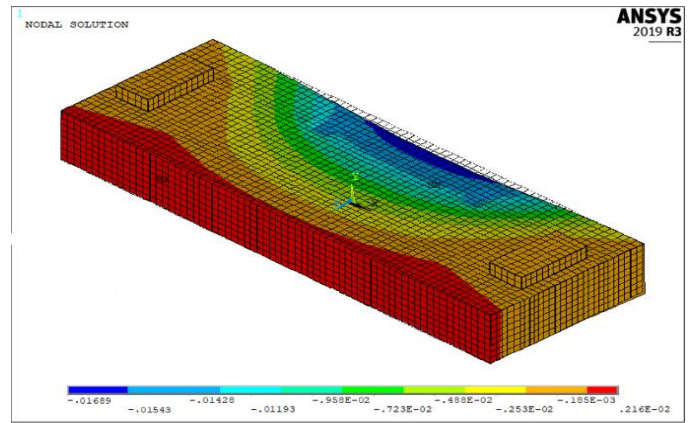
a) Top view
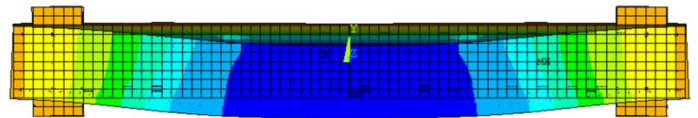
b) Front view

Figure 18. Deformation for specimen B2 - FEM Analysis
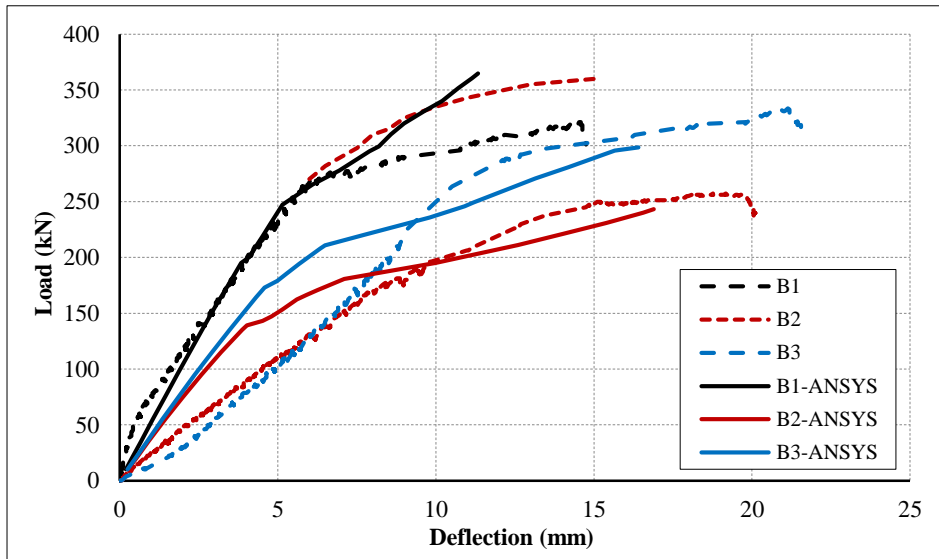
Figure 19. Load deflection curves from experimental and FEM analysis - Group (1)
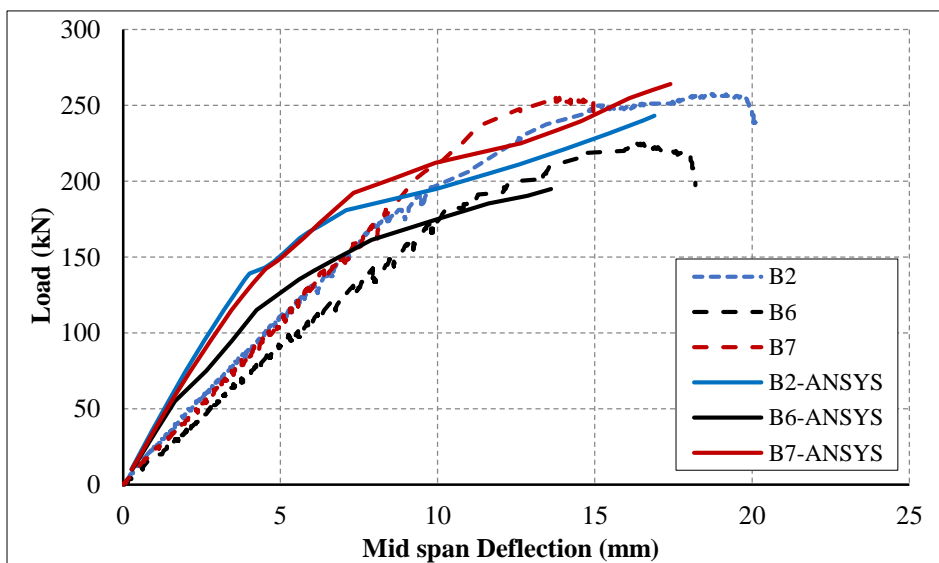
Figure 20. Load deflection curves from experimental and FEM analysis - Group (2)
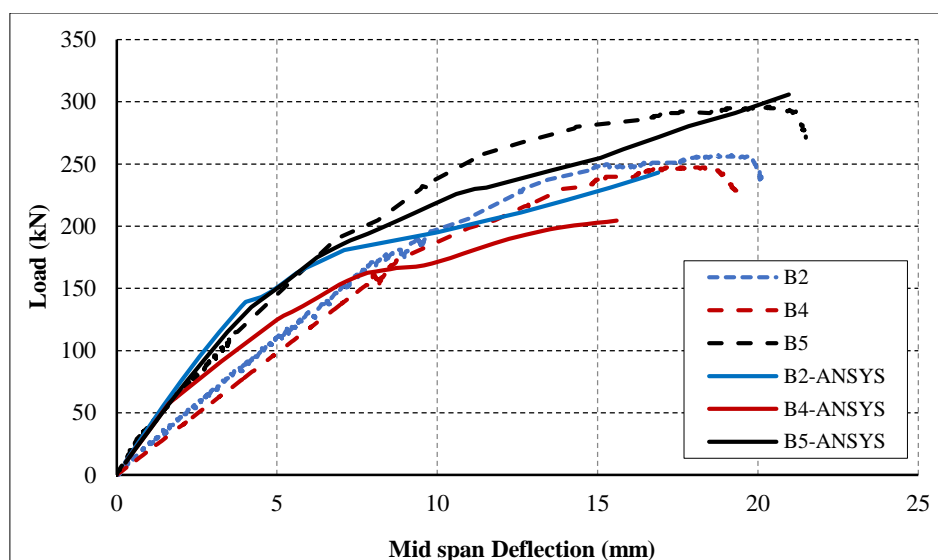
Figure 21. Load deflection curves from experimental and FEM analysis - Group (3)

Table 3 shows the output data for the seven specimens using the ANSYS program [24]. The analytical results gave good correlations with the experimental ones for Beams B2 to B7. However, Beam B1 shows higher values for the cracking load and ultimate failure load compared to the experiment. This confirms what was mentioned before in section 2.2 that the experimental results for Beam B1 are underestimated due to some issues with loading at the time of the experiment. The variation between the ultimate load and deflection at ultimate load between both experiment and analysis was within $\pm$ 24%. It was observed in the FEM analysis results that the longitudinal reinforcement of Beams B1, B2, B3, B4 and B5 reached the yield limit before the concrete crushing while the longitudinal reinforcement of Beams B6 and B7 did not reach the yield limit. The transverse reinforcement in FEM results did not reach their yield limit. These results follow the same trend as in the experimental output except for Beam B4.

Figures 15 and 16 show the comparison between the cracking patterns at failure for Beams B1 and B2 obtained from the experiment and that obtained from the FEA for both the bottom and the front sides. The cracking patterns follow a very similar pattern between the experiment and the analysis. Figures 17 and 18 show the deformation shape for the two beams obtained from the analysis from two perspectives and the stress distribution across the whole beams. The two figures clearly show the difference between Beam B1 where the eccentricity was taken as zero and Beam B2 with eccentricity 200 mm (e/B = 0.333). The stresses in B1 are highest at the midspan of the beam and have uniform values along the cross section. While for Beam B2 the stresses are highest at the side closer to the load with the direction of stresses changing at the opposite side from the load. The load deflection curves showed good correlations between experimental output and FEA. The load deflection curves for Group (1) are shown in Figure 19 while those for groups (2) and (3) are shown in Figures 20 and 21, respectively.

4.2. Parametric Study

To further understand the behavior of wide shallow beams under eccentric loading, a parametric study was conducted using the Finite element analysis program ANSYS V.19 [24]. Seven more wide shallow beams having the same dimensions as that tested experimentally (L=1700, b=600, t=200, and d=180 mm) were analyzed. The study of the specimens was performed through four groups as shown in Table 4 with the FEM analysis of Beam B2 used as a reference. Group (4) was designed to study the effect of using concrete with higher compressive strengths. It consisted of two beams; B8 and B9, in addition to B2. Group (5) consisted of two beams to study the effect of the ratio of the bottom reinforcement. In this group the reinforcement ratio was changed from 0.74% in Beam B2 to 0.42% for Beam B10 and 0.29% for Beam B11. The value 0.29% was chosen as it is the minimum reinforcement ratio specified for beams by the ECP 203-2018 [25].

As for Group (6), it also consisted of two beams to study the effect of the spacing between stirrups in the longitudinal direction. It has been widely assumed in most of the design codes [25, 26, 29] that the concrete cross section of wide beams is large enough to satisfactorily withstand the shear stresses without shear reinforcement. Previous research [15] however proved that the use of shear reinforcement can be quite beneficial. In addition, recent research, [12] and [28], pointed out that it will be quite difficult to accurately assess the shear capacity of large, lightly reinforced wide members without web reinforcement. This part of the research aims to assess the use of the stirrups and their spacing in case of wide beams subjected to eccentricity in the loading conditions. Maximum values for the spacing between stirrups are set for narrow beams subjected to torsion as 200 mm. However, no reference data can be

found for wide beams subjected to torsion. The values of 50, 75, 100 mm were previously used for the beams in Group (2) and here two more beams with spacing 150 mm and 200 mm are added. Shear reinforcement spacing limitations along the beam length are provided in the design codes as mentioned above, however, few limits exist for appropriate spacing of stirrup legs across the transverse direction [7]. Group (7) – Beam B14 – is used to study the effect of the stirrups spacing in the transverse direction or the number of legs of the stirrups where two legged stirrups having a transverse spacing of 560 mm are used and compared to Beam B2 with four branches stirrups and a transverse spacing of 187 mm. Figure 22 and Table 4 show the details of the Beams B8 through B14.

a) Plan

b) Sectional elevation

c) ross section A-A for beams B8, B9, B12 and B13

d) Cross section A-A for beam B10

e) Cross section A-A for beam B11

f) Cross section A-A for beam B14
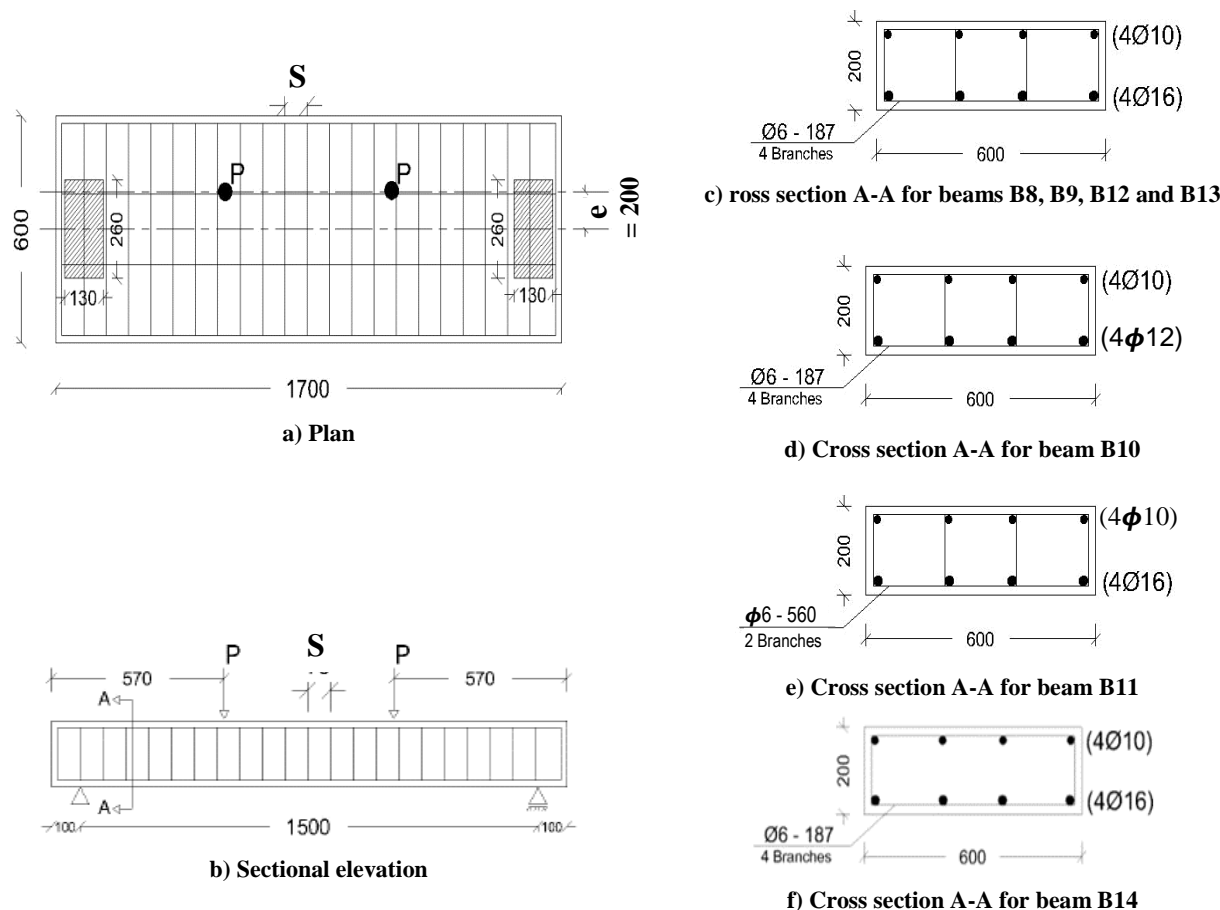
Figure 22. Specimen details for Beams B8 to B14

Table 4. Details of the beam specimens for the parametric study and analysis results

Specimen		Dimensions	Bottom Reinforcement				Stirrups		fcu (MPa)	FEM analysis results		
			Area mm²	D mm	No. of bars	Ratio %	No of branches	S mm		P_u (kN)	Δ_u (mm)	ε_{main} (μ)
ANSYS	B2	600×200×1700 mm, e/b = 0.333, e = 200 mm, e/b = 0.333	804.24	16	4	0.74	Ø6 @ 187 mm 4 branches	75	30	243.2	16.90	2407
Group (4)	B8		804.24	16	4	0.74		75	40	301.7	15.64	2922
	B9		804.24	16	4	0.74		75	50	352.1	16.25	3225
Group (5)	B10		452.16	12	4	0.42		75	30	191.2	15.39	3918
	B11		314.00	10	4	0.29		75	30	171.0	11.43	3610
Group (6)	B12		804.24	16	4	0.74		200	30	139.1	8.89	2549
	B13		804.24	16	4	0.74		150	30	172.0	14.29	3117
Group (7)	B14		804.24	16	4	0.74	Ø6 @ 560 mm 2 branches	75	30	203.0	15.20	3202

fcu: compressive strength of concrete, P_u: Ultimate load, Δ_u: Deflection at ultimate load; ε_{main}: Strain in longitudinal reinforcement at failure.

Effect of the Compressive Strength of Concrete – Group (4)

The three beams in Group (4) were studied having concrete compressive strengths of 30, 40 and 50 MPa. These values represent the common range used in practice for normal strength concrete in addition to one specimen with high strength concrete through the 50 MPa mix. The load deflection curves for Group (4) are shown in Figure 23. Increasing the compressive strength led to a notable increase in the ultimate load capacity where the ultimate load was

increased by 24% when the compressive strength was increased from 30 MPa to 40 MPa and by 45% when the compressive strength was increased to 50 MPa. The increase in the ultimate load of the beams can be linearly related to the concrete compressive strength. However, further study is needed to support this output. No significant change was noticed in the values of deflection where the deflection at ultimate load for B8 and B9 was 15.64 and 16.25 mm, respectively as seen in Table 4.
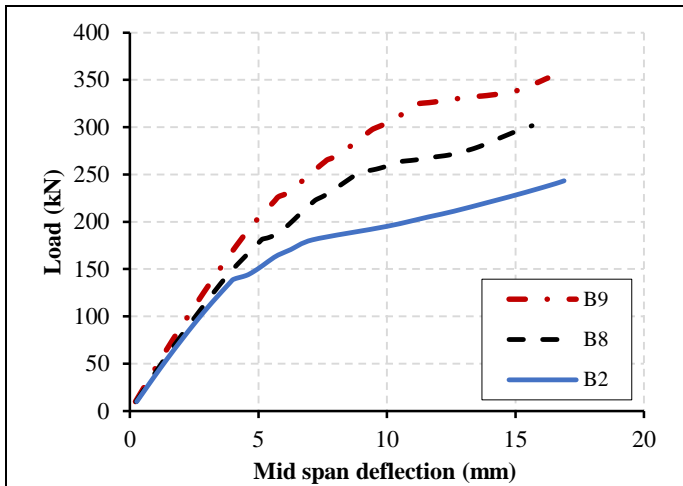
Figure 23. Load-Deflection curves for Group (4)
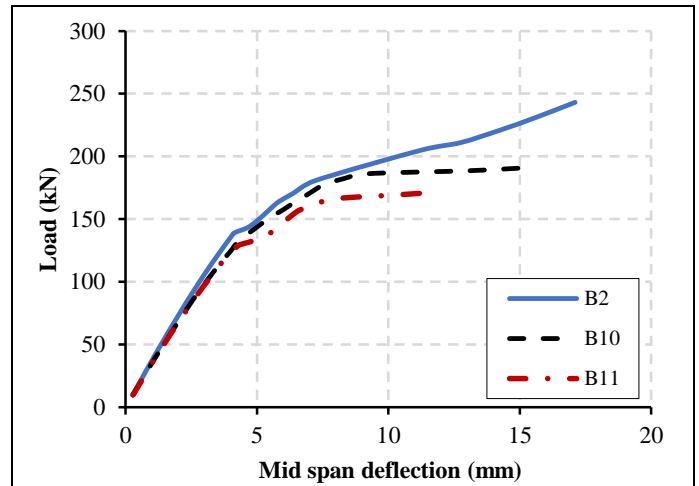
Figure 24. Load-Deflection curves for Group (5)

Effect of the Main Reinforcement Ratio - Group (5)

Figure 24 gives the load deflection curves for Group (5). A reduction in the ultimate load capacity of 21% and 30% was seen when the reinforcement ratio was reduced to 0.42% and 0.29%, respectively. In addition, ductility was reduced with the decrease in the main reinforcement ratio as the values of the deflection at ultimate load decreased by 8% for Beam B10 and more notably for Beam B11 by 32%.

Effect of the Longitudinal Spacing between Stirrups - Group (6)

Group (6) is an extension of Group (2) where more values for the spacing between stirrups were studied. Previously spacing values of 50, 75, 100 mm were used. Here, two more values were added; 150 mm for B13 and 200 mm for B12. The load deflection curves can be seen in Figure 25. The curves for the beams in this group are plotted with the analysis output for Beam B4 and Beam B5 as well as Beam B2 for reference. As the longitudinal spacing between stirrups decreased, the ductility and the ultimate capacity of the beam increased. Figure 26 shows the values of the ultimate load against the ratio of s/d for the five beams where s denotes the longitudinal spacing between the stirrups and d is the depth of the beam. The ultimate load decreases sharply up to s/d = 0.5 while for values large than that the slope of the curve is reduced. It should be noted here that s/d = 0.5 is the limit set by most codes [25, 26] for the maximum spacing between stirrups. The curve plotted in Figure 26 supports this stipulation as the ultimate load capacity is largely reduced up to s/d = 0.5. Increasing s more than 0.5d could lead to excessive loss in the ultimate capacity of the beam.
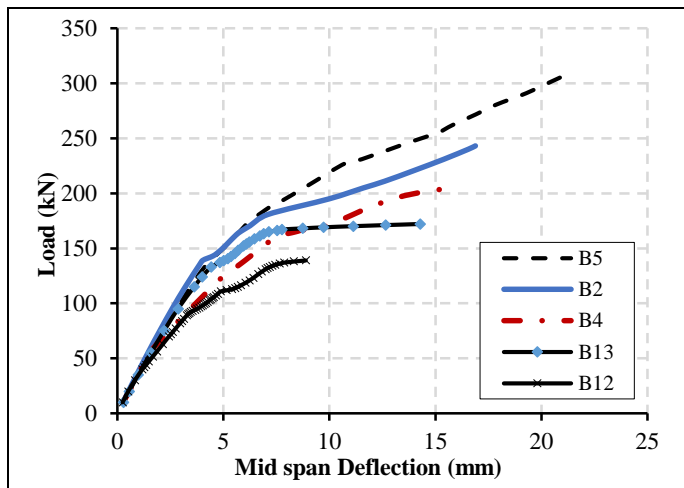
Figure 25. Load-Deflection curves for Group (6)
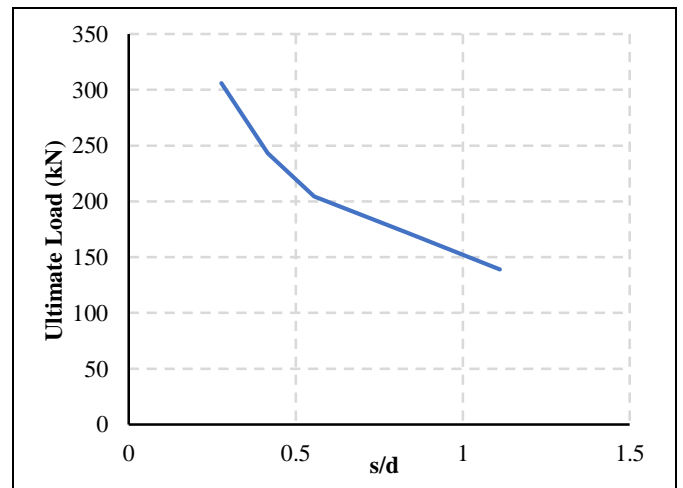
Figure 26. Effect of the longitudinal spacing between stirrups

Effect of the Stirrups Leg Spacing (Transverse Spacing) - Group (7)

Group (7) aims to study the effect of the transverse spacing of the stirrups. Design codes have different guidelines for the limits for the transverse spacing. Eurocode 2 [29] puts a limit of 0.75 d or 600 mm which is the same as that for the longitudinal spacing while ECP 203-2018 [25] has a maximum limit of 250 mm. On the other hand, the ACI 318-19 [26] gives no limit for the value of the transverse spacing. The load deflection curves for Group (7) are shown in Figure 27. Beam B14 is compared with Beam B2 where the number of branches of stirrups was changed from 4 to 2 corresponding to a change of leg spacing from 187 mm to 560 mm. A reduction in the ultimate load capacity of 16.5% was seen and the mid span deflection was reduced by 10%.
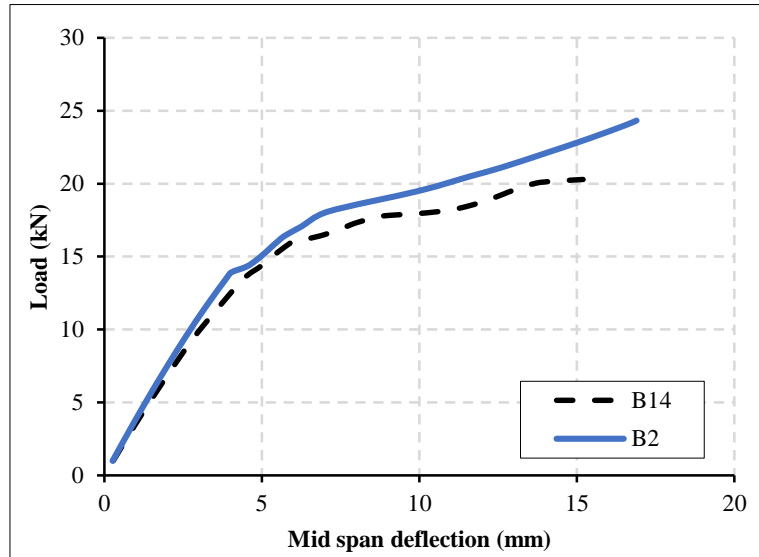
Figure 27. Load-Deflection curves for Group (7)

5. Conclusions

A combined bending torsion experiment on wide shallow RC beam specimens was conducted. This paper presents the details of the experiment and the experimental results for seven beam specimens under eccentric loading. In addition, the experimental results were compared with the analytical results obtained using the finite element program ANSYS 19 followed by an extended analytical study to investigate the effect of various parameters on the behavior of wide shallow beams under eccentric loading.

Based on the results obtained in this research, the following points can be concluded:

- Applying vertical load with varying eccentricities to RC wide beams exerts torsional moments in addition to the bending and shear stresses which can be clearly seen in the cracking patterns and failure modes.

- Increasing the load eccentricity from 100 to 200 mm (Approx. 17 to 33% of the beam width) leads to a decrease in ultimate load capacity. Based on the results of the experimental program a decrease of 21% was obtained. In addition, a decrease in the stiffness and toughness of 19 and 16% was obtained due to an increase in the torsional stresses along the beam cross section.

- Beams with small load eccentricity (0.167) behave in a way similar to beams without any load eccentricity.

- Decreasing the spacing between stirrups helps in controlling the cracks width and increasing the ultimate load. The ultimate load capacity was almost doubled when the spacing to depth ratio (s/d) was decreased from 1 to 0.28. Ductility is also improved with the lower longitudinal spacing between stirrups.

- The arrangement and distribution of longitudinal steel reinforcement affects the behavior of the wide beams even when having the same reinforcement ratio. It can be rationalized that the cracking moment of inertia is the main factor governing the effect of the reinforcement distribution.

- Using uniform distribution of longitudinal bars with a large diameter leads to an improved behavior compared to using a small diameter keeping the same reinforcement ratio of steel. However, concentration of longitudinal reinforcement under the applied load increases the ultimate load capacity but decreases the ductility of the specimen.

- The modeling of the wide RC beams under eccentric loading using the finite element program ANSYS proved to be effective where good agreement was found between the output of the analytical program and the experimental results.

- Using high strength concrete increases the torsional capacity of wide beams and increases the ultimate load capacity. An increase of approximately 25% was obtained when compressive strength was increase to 40 N/mm² from the original 30 N/mm² and of approximately 46% for compressive strength of 50 N/mm².

- Decreasing the ratio of the main longitudinal reinforcement leads to a noticeable decrease in ultimate load capacity and the ultimate deflection.

- The transverse spacing between stirrups legs across the width of the wide beam affects the beam behavior. This was noticed when changing the shape of transverse reinforcement from four branches to two branches thus leading to a decrease in the torsional resistance and the ultimate load capacity by approximately 16.5%.

6. Declarations

6.1. Author Contributions

The main ideas and the methodology of the research were discussed and decided by all authors. The manuscript was written by S.M. and R.M. and review was done by M.K. The results, discussions, interpretation, and conclusion were completed by all authors. All authors have read and agreed to the published version of the manuscript.

6.2. Data Availability Statement

The data presented in this study are available in article.

6.3. Funding

The authors received no financial support for the research, authorship, and/or publication of this article.

6.4. Conflicts of Interest

The authors declare no conflict of interest.

7. References

[1] Helou, Samir H, and Munther Diab. "Slabs with Hidden Beams, Facts and Fallacies." In The International Conference of Civil Engineering (ICCE), 02:316–19, 2014.

[2] Hsu, Thomas TC. "Torsion of Structural Concrete-Plain Concrete Rectangular Sections." Special Publication, American Concrete Institute 18 (1968): 203-238.

[3] Wang, Guo Lin, and Wen Sheng Ding. "Experimental Study on Shear Behavior of Prestressed Concrete Beams." Applied Mechanics and Materials 226–228 (November 2012): 1045–1048. doi:10.4028/www.scientific.net/amm.226-228.1045.

[4] Said, M., and T.M. Elrakib. "Enhancement of Shear Strength and Ductility for Reinforced Concrete Wide Beams Due to Web Reinforcement." HBRC Journal 9, no. 3 (December 2013): 235–242. doi:10.1016/j.hbrcj.2013.05.011.

[5] Mohammadyan-Yasouj, S. E., A. K. Marsono, R. Abdullah, and M. Moghadasi. "Wide Beam Shear Behavior with Diverse Types of Reinforcement." ACI Structural Journal 112, no. 2 (2015): 199–208. doi:10.14359/51687299.

[6] Lee, K S, S H Lee, and S W Shin. "Shear Behavior of Reinforced Concrete." MSc. Thesis, Faculty of Engineering, Cairo University, Giza, Egypt (2013).

[7] Lubell, Adam S., Evan C. Bentz, and Michael P. Collins. "Shear Reinforcement Spacing in Wide Members." ACI Structural Journal 106, no. 2 (2009): 205–14. doi:10.14359/56359.

[8] Shuraim, Ahmed B. "Transverse Stirrup Configurations in RC Wide Shallow Beams Supported on Narrow Columns." Journal of Structural Engineering 138, no. 3 (2012): 416–24. doi:10.1061/(asce)st.1943-541x.0000408.

[9] Elansary, Ahmed A., Yasser Y. Elnazlawy, and Hany A. Abdalla. "Shear Behaviour of Concrete Wide Beams with Spiral Lateral Reinforcement." Australian Journal of Civil Engineering (June 23, 2021): 1–21. doi:10.1080/14488353.2021.1942405.

[10] Angelakos, Dino, Evan C. Bentz, and Michael P. Collins. "Effect of Concrete Strength and Minimum Stirrups on Shear Strength of Large Members." ACI Structural Journal 98, no. 3 (2001): 290–300. doi:10.14359/10220.

[11] American Concrete Institute, Detroit, Building Code Requirements for Reinforced Concrete (ACI 318-63) - ACI Committee 318. Farmington Hills, Mich, (1989).

[12] Sherwood, Edward G., Adam S. Lubell, Evan C. Bentz, and Michael P. Collins. "One-Way Shear Strength of Thick Slabs and Wide Beams." ACI Structural Journal 103, no. 6 (2006): 794–802. doi:10.14359/18229.

[13] ACI Committee 318. "Building Code Requirements for Structural Concrete (ACI 318-05) and Commentary (318R-05)." American Concrete Institute, Farmington Hills, Mich., (2005): 430.

[14] Kim, Min Sook, Joowon Kang, and Young Hak Lee. "Improved Shear Strength Equation for Concrete Wide Beams." Applied Sciences (Switzerland) 9, no. 21 (2019): 4513. doi:10.3390/app9214513.

[15] Collin, Michael P., Phillip T. Quac, and Evan C. Ben. "Shear Behavior of Thick Slabs." ACI Structural Journal 117, no. 4 (2020): 115–26. doi:10.14359/51724666.

[16] ACI Committee 318. "Building Code Requirements for Structural Concrete (ACI 318-14) and Commentary (318R-14)." American Concrete Institute, Farmington Hills, Mich., (2005): 519.

[17] Bernardo, Luis F.A., and Sérgio M.R. Lopes. "Torsion in High-Strength Concrete Hollow Beams: Strength and Ductility Analysis." ACI Structural Journal 106, no. 1 (2009): 39–48. doi:10.14359/56282.

[18] Elnady, Ahmed Mamdouh. "Torsional behavior of RC beams with opening retrofitted with FRP material." MSc. Thesis, Faculty of Engineering, Zagazig University, Egypt, (2015).

[19] Fang, I. Kuang, and Jyh Kun Shiau. "Torsional Behavior of Normal- and High-Strength Concrete Beams." ACI Structural Journal 101, no. 3 (2004): 304–13. doi:10.14359/13090.

[20] Kim, Yail J., Yongcheng Ji, and Troy Butler. "Uncertainty Modeling of Carbon Fiber-Reinforced Polymer-Confined Concrete in Acid-Induced Damage." ACI Structural Journal 116, no. 6 (2019): 97–108. doi:10.14359/51716761.

[21] Lee, Jung Yoon, Kil Hee Kim, Seung Hoon Lee, Changhyuk Kim, and Min Ha Kim. "Maximum Torsional Reinforcement of Reinforced Concrete Beams Subjected to Pure Torsion." ACI Structural Journal 115, no. 3 (2018): 749–60. doi:10.14359/51701108.

[22] Jeng, Chyuan Hwan, Sheng Fu Peng, Hao Jan Chiu, and Chih Kun Hsiao. "New Torsion Experiment on Large-Sized Hollow Reinforced Concrete Beams." ACI Structural Journal 111, no. 6 (2014): 1469–80. doi:10.14359/51687166.

[23] Ju, Hyunjin, and Deuckhang Lee. "Nonlinear Analysis of Reinforced Concrete Members Subjected to Combined Torsion and Bending Moment." ACI Structural Journal 118, no. 4 (2021): 55–70. doi:10.14359/51732643.

[24] ANSYS, (2019), Release 14.0 Documentation. ANSYS Inc.

[25] ECP 203-2018. "The Egyptian Code for Design and Construction of Concrete Structures." Ministry of Housing, Cairo, Egypt, (2018).

[26] ACI Committee 318. "Building Code Requirements for Structural Concrete (ACI 318-19) and Commentary (318R-19)." American Concrete Institute, (2019).

[27] BS 8110-2015 "Structural Use of Concrete: Part 1: Code of Practice for Design and Construction." BRITISH STANDARD.

[28] Lubell, Adam, Ted Sherwood, Evan Bentz, and Michael Collins. "Safe Shear Design of Large Wide Beams." Concrete International 26, no. 1 (2004): 66–78.

[29] Eurocode 2, "Design of Concrete Structures—Part 1-1: General Rules and Rules for Buildings (EN1992-1-1)." European Committee for Standardization, Brussels, Belgium, (Dec. 2004): 225.